Detection and influence of shrinkage pores and non-metallic inclusions on fatigue life of cast aluminum alloys

Yakub Tijani[1], Andre Heinrietz[1], Wolfram Stets[2], Patrick Voigt[2]

[1]Fraunhofer-Institut für Betriebsfestigkeit und Systemzuverlässigkeit LBF, Bartningstr. 47, 64289 Darmstadt, Germany
[2]Institut für Gießereitechnik gGmbH, Sohnstraße 70, 40237 Düsseldorf, Germany

Keywords: Aluminum, Shrinkage Pores, Fatigue Strength

Abstract

In this work, test bars of cast aluminum alloys EN AC-AlSi8Cu3 and EN AC-AlSi7Mg0.3 were produced with a defined amount of shrinkage pores and oxides. For this purpose a permanent mold with heating and cooling devices for the generation of pores was constructed. The oxides were produced by a contamination of the melt. The specimens and their corresponding defect distributions were examined and quantified by X-Ray computer tomography (CT) and quantitative metallography respectively. A special test algorithm for the simultaneous image analysis of pores and oxides was developed. The defective samples were examined by fatigue testing. The presence of shrinkage pores causes a lowering of the fatigue strength. The results show that pore volume is not sufficient to characterize the influence of shrinkage pores on fatigue life. A parametric model for the calculation of fatigue life based on the pore parameters obtained from CT scans was implemented. The model accounts for the combined impact of pore location, size and shape on fatigue life reduction.

Introduction

The most of aluminum castings are used in automotive applications that require high mechanical cyclic loading. However, during the production and processing of aluminum alloy melt, several kinds of defects in various forms are generated. The defects lead to microstructural discontinuities and adversely influence the structural durability of the produced castings [1, 2]. Typical example of cast defects are shrinkage pores which are often correlated with the release of solved gas in the solidifying melt [3, 4]. Another type is non-metallic inclusions (in most cases oxide skins) which are generated due to the charging material in the furnace or during mold filling [5]. These defects cannot be completely avoided during production without incurring additional costs. Furthermore the consideration of quantitative defect parameters in the numerical analysis of fatigue life is not state of the art. Another problem is the quantitative analysis of the content and distribution of the inner defects in Al castings. The metallographic investigation by image analysis is a standard tool for materials testing but the simultaneous distinction of several defects at the same time is not possible with most commercial software packages.

Experimental Procedure

Design of the permanent mold

The precondition for the investigation of the influence of defect on fatigue life is the reproducible production of test samples with defined defect content and volume. This demands

defined conditions during the mold filling and solidification, which must remain constant during each casting cycle. The mold should be able to control the cooling conditions for the adjustment of a defined solidification and the generation of defined shrinkage pores. By simulating the required conditions, permanent test molds were constructed. For this purpose, the molds were equipped with thermocouples, heating elements and cooling channels. As indicated in Figure 1, the molds were designed with vertically orientated, upward cast test bars for low pressure die casting and gravity casting.

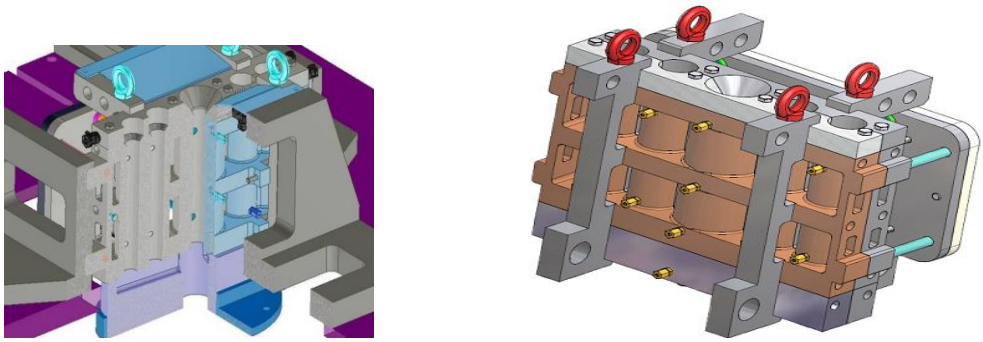

Figure 1. Designed permanent mold with downsprue and runner for (a) low pressure die casting and (b) gravity casting

The regulation of the solidification condition was furthermore changed by the application of isolating and graphite coatings with different thermal conductivities. First tests showed that it is possible to cast samples with a high thermal gradient (low shrinkage pores) and with a lower thermal gradient (worse feeding with a resulting higher amount of shrinkage pores).

Casting trials

Several preliminary trials were conducted to select the right casting conditions. The temperature of the melt, the temperature distribution in the permanent mold and the pouring time were varied. Subsequently, fatigue test specimens were cast. This paper will present only the results of the low pressure die casting. The cast parameters are given in table 1.

Table 1. Cast parameters for the low pressure die casting

Cast alloys	EN AC-AlSi8Cu3 and EN AC-AlSi7Mg0.3
Melt temperature	750 °C
Pouring temperature	730 °C
Filling time	5 s
Pressure for feeding	10-30 mbar
Mold temperature at the beginning of cast	375 °C
Mold temperature at the opening	490 °C

The cast conditions were adjusted to generate lower, medium and high levels of porosities. One special method was to put metallic inserts on the top of the test bar cavity for worsening of the feeding behavior. One part of the melt was cleaned by impellering and the other part of the melt was impurified by addition of annealed turnings or impurified ingots. The latter procedure leads to production of melts with non-metallic inclusions. However, the production of specimens with oxide inclusions was not reproducible. The amount and the distribution of the oxide skins or compact inclusions were non-uniformly distributed in the produced test samples.

The cast test specimens were heat treated; T5 for EN AC-AlSi8Cu3 and T6 for EN AC-AlSi7Mg0.3. Furthermore, continuous cast ingots were included as reference material.

Classification of the defects

X-ray computer tomography

All cast samples (a total of 1092 bars) were investigated by X-ray computer tomography (CT). A fan-beam CT with an accelerating voltage of 420 keV was used. The single investigation of one test bar (diameter 12 mm) allows the detection of pores with more than 0.1 mm diameter. Because of the necessity to test a higher amount of samples at the same time (30 bars at one holding device), a lower limit of detectability of about 0.5 mm was achieved. The results of these CT investigations, see figure 2, were the basis for the final selection of test samples and their classification into three groups. The classification was based on the largest volume of shrinkage pore (i.e. pore volume, PV < 0.5mm^3, 0.5 – 2 mm^3 and 2 – 4 mm^3). The CT results showed a high scattering of the maximum pore volume also in test series with comparable conditions. Finally, only 16 % of all test bars were selected for fatigue investigation. Few selected samples were additionally investigated by micro focus CT for the generation of a detailed 3D model of the shrinkage pores. These data serve as basis for the later FEM simulation.

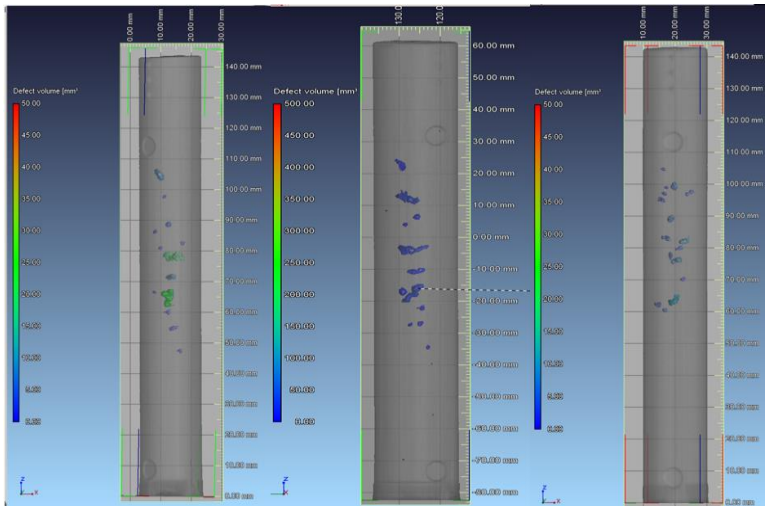

Figure 2: Reconstructed X-ray computer tomography (CT) for classification of shrinkage pores

Fatigue experiments

Fatigue experiments were carried-out on the specimens by using a 25 kN servo-hydraulic

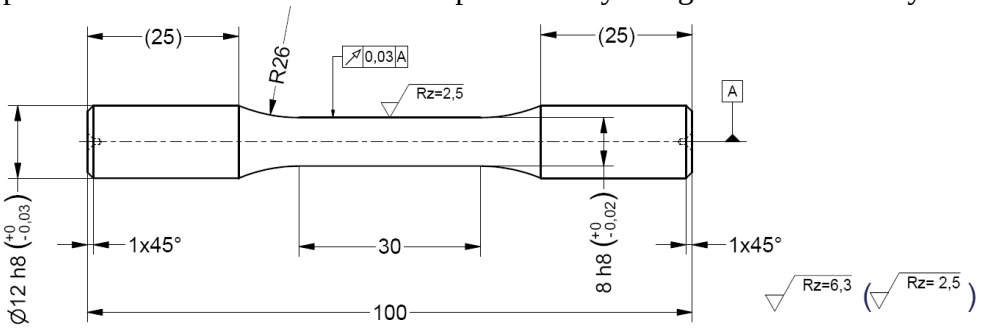

Figure 3. Specimen geometry for fatigue experiments

machine. The stress-controlled tests were conducted under a fully reversed constant-amplitude axial loading with stress ratio R = -1. The test frequency was 80 Hz. Figure 3 shows the specimen geometry used for the investigation (EN ISO 1302).

Results and Discussion

Metallographic examination

The detection or quantification of non-metallic inclusions with the CT technique was not possible because of the low thickness of these defects (few µm). An algorithm has been developed for this purpose allowing an automatic image analysis of defects in Aluminum cast alloys. The basis for this development was the preparation of microscopic specimen from the produced melts and the production of pictures with 148 individual defects. Predominantly these defects were shrinkage pores, gas pores and oxides, see figure 4. A board of 8 experienced specialists judged the images and divided the defects into three categories. From each individual defect the shape factor, the fiber thickness and the ratio of fiber thickness to the length was analyzed [6]. Using these features combined with the expert findings, a classifier for the automatic separation and quantification of shrinkage pores, gas pores and oxide inclusions was created. The application of this algorithm in the investigation of 3000 defects in several images gave a hit rate of 90 %.

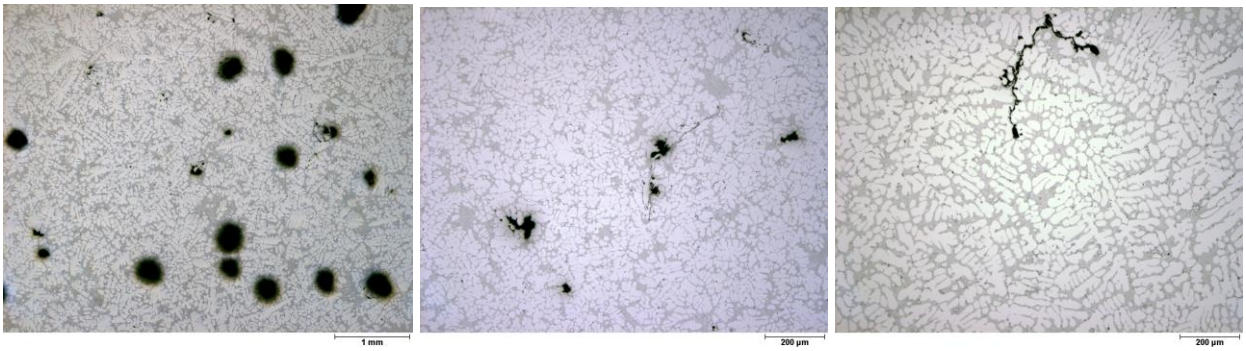

Figure 4. Gas pores, shrinkage pores and oxide inclusions (skins) in Al cast samples (from left to right)

Fractography

The tested samples were investigated by light microscope and by scanning electron microscope. In 95% of the cases, a shrinkage pore was crack-initiating, see figure 5. Only 5% of the samples showed oxide inclusions as crack-initiating. This is consistent with the hierarchical nature of crack-initiating defects; in the presence of shrinkage pores and oxide, the crack will mostly be initiated by the shrinkage pores [7]. In 96% of the AlSi8Cu3 samples, the crack initiators were situated at the machined sample surface (cut pores). The AlSi7Mg0.3 samples have only 69 % crack initiators at the surface, the rest were inside the specimen. The reason for this difference is probably the higher ductility of AlSi7Mg0.3 (A = 8.7 %) in comparison to AlSi8Cu3 (0.9 %).

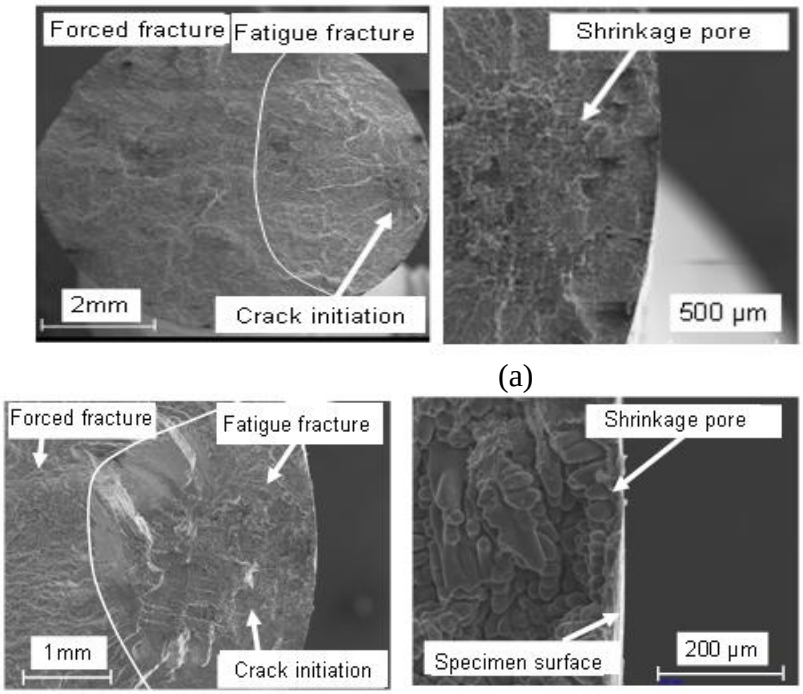

Figure 5. Scanning Electron Microscope images of (a) AlSi8Cu3 and (b) AlSi7Mg0.3 specimens showing the fracture surface, location of crack initiation and the shrinkage pore that initiated the crack.

Fatigue Results

The stress-cycles diagrams, S-N curves, of the low pressure die cast specimens are shown in figure 6 and figure 7 for both AlSi8Cu3 and AlSi7Mg0.3 alloys. In figure 6, the scatter of the test series with defects are significantly higher than the scatter of the reference material in both alloys. A reduction of 40% and 8.5% in fatigue strength is observed at $N=10^7$ for AlSi8Cu3 and AlSi7Mg0.3 respectively. In figure 7, the three classes of specimens based on maximum pore volumes are shown. For AlSi8Cu3, the fatigue strength (at $N=10^7$) of the specimens with maximum volume < 0.5 mm^3 has the highest strength in comparison to the other two classes which show no significant difference. For AlSi7Mg0.3, the S-N curves of the three classes overlap and the slopes of the curves decrease with increasing maximum pore volume.

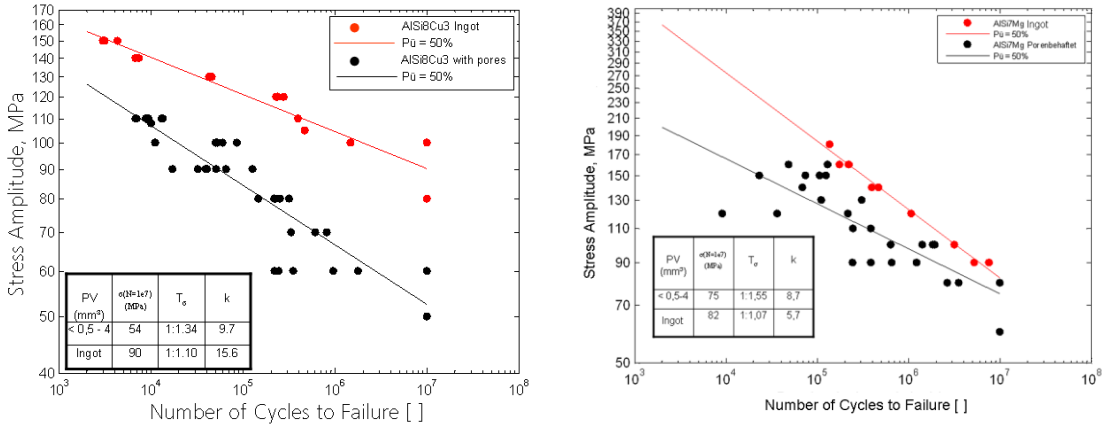

Figure 6. S-N curves of specimens with pores (black) and reference material (red) for AlSi8Cu3 (a) and AlSi7Mg0.3 (b).

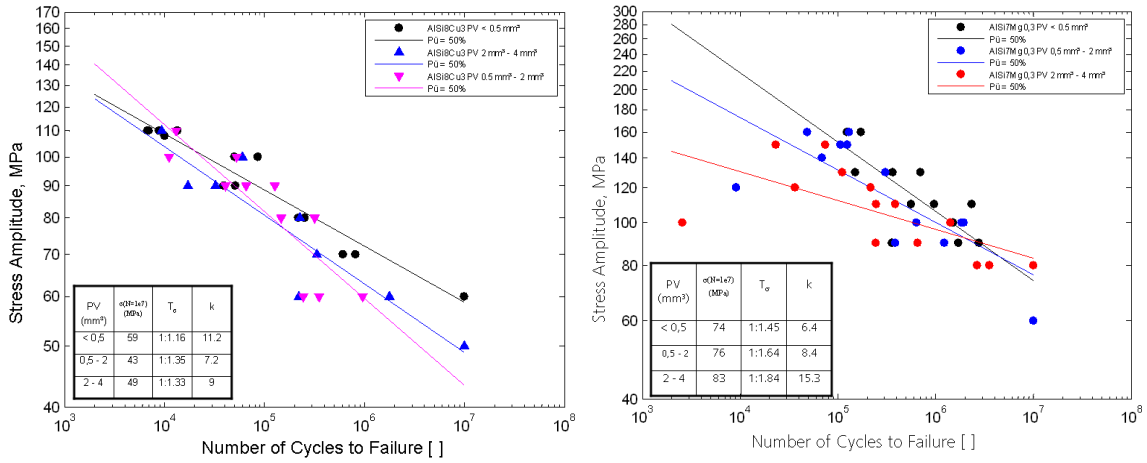

Figure 7. S-N Curves of the specimens with different maximum pore volumes (PV) for AlSi8Cu3 (a) and AlSi7Mg0.3 (b).

Parameterized Model for the calculation of cycle life

A parameterized evaluation model to determine the notch shape factor of a pore in relation to its size, shape and distance to the surface has been developed [8]. With this model it is possible to calculate fatigue life of pore-prone specimens on the basis of linear elastic material properties, the parameterized model and the pore parameters determined from computed tomography (CT). The model correlates well -from the point of view of stress mechanics- with the FEM-calculations of pore-prone samples based on micro CT data. For the application of this model it is necessary to extract image analytical parameters of the pores from the CT scans. In general, the influence of pores on the local stress in the cast aluminum alloy samples were investigated by finite element method. The reconstructed pores were triangulated and exported for finite element analysis using Abaqus software [9]. A linear elastic calculation was carried-out with nominal stress of 90 MPa. A model of the specimen AlSi7Mg0.3-T6 containing a shrinkage pore is shown in Figure 8. The maximum principal stress at the pore is 571.7 MPa. It was observed that the highest stresses occur at the pores in the regions between the pores and the specimen surface. The pore proximity to the surface also plays a significant role: the closer the pores are to the surface, the higher are the calculated local stresses.

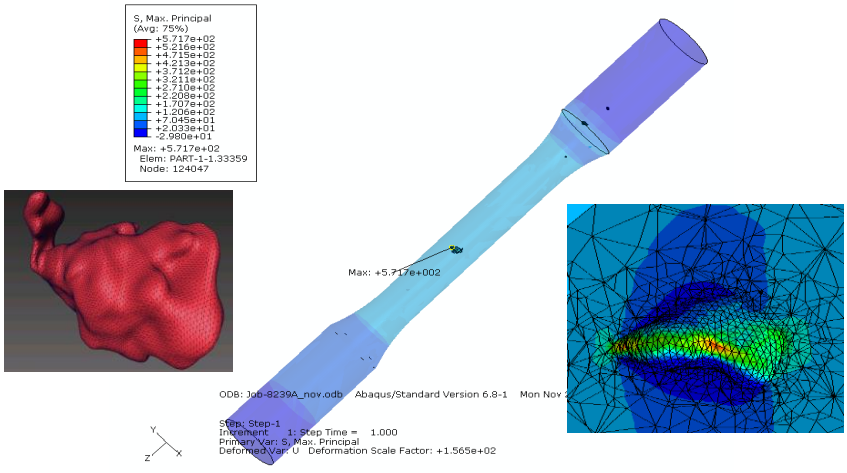

Figure 8. Finite element model of a specimen from AlSi7Mg0.3-T6 showing the pore with highest value of maximum principal stress

From the finite element analysis of several specimens containing pores, the notch shape factors K_t of the pores were determined:

$$K_t = \frac{1}{\eta}\left(2.74 + 0.6R - \frac{0.71R}{\sqrt{R} - \frac{1.1}{\sqrt{R}} - R} + \frac{0.31}{\sqrt{R}} - 2.21\sqrt{R}\right)\frac{Diameter}{\left(\frac{6.Volume}{Area}\right)} \qquad (1)$$

where $R = \frac{\text{pore diameter}}{\text{pore distance to surface}}$ $(R \neq 0)$.

In Figure 8, the computed notch shape factor of the shrinkage pore in relation to its size, shape and distance to the specimen surface is 6.4. By using the parameterized evaluation model in Equation 1, the notch shape factor of the shrinkage pore is found to be 6.9. The fatigue life of a pore-prone specimen N_{pore} can be expressed as

$$N_{pore} = \frac{N_k}{\left(\frac{\sigma_{pore} K_{f(pore)}}{\sigma_k}\right)^k} \qquad (2)$$

where N_k and σ_k are the number of cycles and corresponding fatigue strength of a pore-free specimen, K_f is the fatigue notch factor (calculated as a function of notch shape factor of the pore and notch sensitivity of the material).By using equations 1 and 2, fatigue life of some specimens were calculated. Figure 9 shows a correlation plot between the calculated fatigue life and the experimental result.

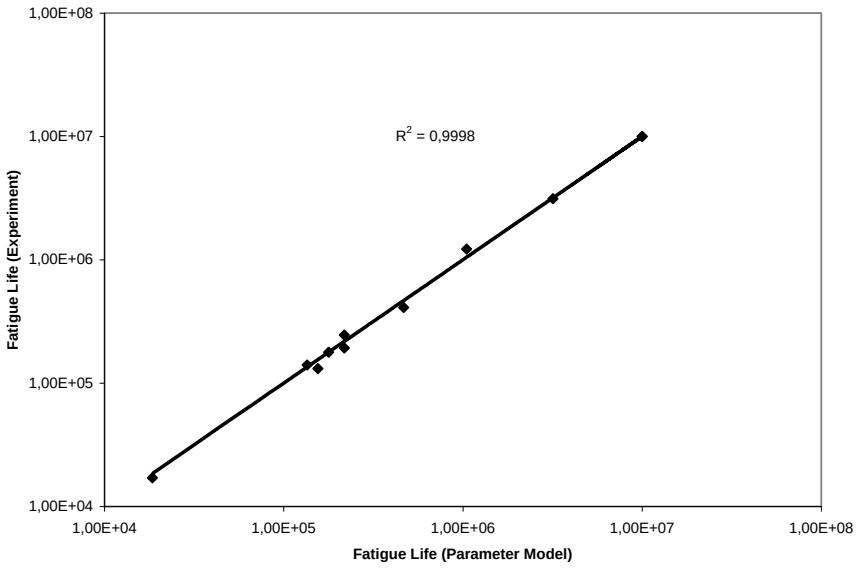

Figure 9. Correlation between results of fatigue life from experimental investigations and the parameterized evaluation model

Conclusions

This work provides a greater understanding of the physical processes which govern the formation of microstructure inhomogeneities and their influence on the fatigue life of material made from cast aluminum alloys. The fatigue experiments indicate that the presence of defects reduces the fatigue strength. However, the results of the fatigue experiments indicate that only the pore volume is not sufficient to quantify the influence of defects on fatigue properties of the material. The implemented parameter model indicated that a comprehensive evaluation will require the pore size, shape and distance to specimen surface, as well as the material behaviour of the alloy. In addition to the experimental investigations, the parameter model provides reliable predictions over the range of conditions found in industrial castings, where pores are among the major driving forces for reduction of structural durability.

Acknowledgments

The presented work is a part of the research project AiF 295 ZN sponsored by the German Federation of Industrial Research Associations (AiF) under the program for the promotion of joint industrial research and development (IGF).

The original publication of this article is shown in the Metallurgical and Materials Transactions Volume 44A, Number 6, June 2013

References

[1] J.Z. Yi, Y.X. Gao, P.D. Lee, H.M. Flower, and T.C. Lindley, The effects of microstructure and defects on fatigue properties in cast A356 aluminium -silicon alloy, Fatigue and Fracture of Engineering Materials and Structures 27 (2004), S. 559 – 570

[2] M.J. Couper, A.E. Neeson, and J.R. Griffiths, Casting Defects and the Fatigue Behaviour of an aluminium Casting Alloy, *Fatigue Fract. Engng. Mater. Struct*. Vol.13 (3), 1990, p 213-227

[3] C.M. Sonsino and J. Ziese, Fatigue Strength and Applications of Cast Aluminium Alloys with different Degrees of Porosity, *Int. J. Fatigue*, Vol 15 (No. 2), 1993, p 75-84

[4] J. Linder, M. Axelsson, and H. Nilsson, The influence of porosity on the fatigue life for sand and permanent mould cast aluminium, International Journal of Fatigue 28 (2006), S. 1752-1758

[5] Q.G. Wang, C.J. Davidson, J.R. Griffiths, and P.N. Crepeau, Oxide Films, Pores and the Fatigue Lives of Cast Aluminum Alloys, Met. & Mat. Trans. B, Vol 37B, Dec 2006, 887-895

[6] A. Velichko, Quantitative 3D Characterization of Graphite Morphologies in Cast Iron using FIB Microstructure Tomography, PhD Thesis, Univ. of Saarland, Germany, 2008, p 114-115

[7] Q.G. Wang, D. Apelian, and D.A. Lados, Fatigue Behaviour of A356-T6 Aluminium Cast Alloys. Part 1. Effect of Casting Defects, *Journal of Light Metals*, Vol 1, 2001, p 73-84

[8] Y. Tijani, A. Heinrietz, T. Bruder, and H. Hanselka, Quantitative Evaluation of Fatigue Life of Cast Aluminium Alloys by Non-Destructive Testing and Parameter Model, Conf. Proc., Mat. Sci. & Techn. 2011, Columbus OH, 2011

[9] Abaqus/CAE, Finite Element Modeling, Visualization and Process automation, Dassault Systèmes (SIMULIA), USA.